Drug Design, Development and Therapy

Dovepress
open access to scientific and medical research

Open Access Full Text Article

ORIGINAL RESEARCH

The Underling Mechanisms Exploration of *Rubia cordifolia* L. Extract Against Rheumatoid Arthritis by Integrating Network Pharmacology and Metabolomics

Weiya Zeng[1–3], Yuan Fang[1–3], Suifen Mo[1–3], Caihong Shen[1–3], Huiling Yang[1–3], Guihua Luo[1–3], Luhua Xiao[1–3], Ruoting Zhan[1–3], Ping Yan[1–3]

[1]College of Traditional Chinese Medicine, Guangzhou University of Chinese Medicine, Guangzhou, People's Republic of China; [2]Key Laboratory of Chinese Medicinal Resources from Lingnan (Guangzhou University of Chinese Medicine), Ministry of Education, Guangzhou, People's Republic of China; [3]Joint Laboratory of Nation Engineering Research Center for the Pharmaceutics of Traditional Chinese Medicines, Guangzhou, People's Republic of China

Correspondence: Ruoting Zhan; Ping Yan, Guangzhou University of Chinese Medicine, No. 232, Outer Ring East Road, Guangzhou, Guangdong, People's Republic of China, Tel/Fax +86 20-39358045, Email ruotingzhan@vip.163.com; yanping@gzucm.edu.cn

Purpose: *Rubia cordifolia* L. (RC) is a classic herbal medicine for the treatment of rheumatoid arthritis (RA) and has been used since ancient times. The ethanol extract of *Rubia cordifolia* L. (RCE) showed obvious anti-RA effects in our previous study. However, further potential mechanisms require more exploration. We aimed to investigate the mechanism of RCE for the treatment of RA by integrating metabolomics and network pharmacology in this study.

Methods: An adjuvant-induced arthritis (AIA) rat model was established, and we evaluated the therapeutic effects of RCE. Metabolomics of serum and urine was used to identify the differential metabolites. Network pharmacology was applied to determine the key metabolites and potential targets. Finally, the potential targets and compounds of RCE were verified by molecular docking.

Results: The results indicated that RCE suppressed foot swelling and alleviated joint damage and also had anti-inflammatory properties by inhibiting the expressions of tumor necrosis factor (TNF)-α, Interleukin (IL)-1β, prostaglandin E2 (PGE2), and P65. Ten and seven differential metabolites were found in the serum and urine, respectively, of rats. Six key targets, ie, phospholipase A2 group IIA (PLA2G2A), phospholipase A2 group X (PLA2G10), cytidine deaminase (CDA), uridine-cytidine kinase 2 (UCK2), charcot-leyden crystal galectin (CLC), and 5′,3′-nucleotidase, mitochondrial (NT5M), were discovered by network pharmacology and metabolite analysis and were found to be related to glycerophospholipid metabolism and pyrimidine metabolism. Molecular docking confirmed that the favorable compounds showed affinities with the key targets, including alizarin, 6-hydroxyrubiadin, ruberythric acid, and munjistin.

Conclusion: This study revealed the underlying mechanisms of RCE and provided evidence that will allow researchers to further investigate the functions and components of RCE against RA.

Keywords: inflammtion, AIA rats, molecular docking, chronic disease

Introduction

Rheumatoid arthritis (RA) is an autoimmune system disorder disease characterized by swollen joints, bone erosion and cartilage deterioration,[1] RA not only damages the joints but also the heart, kidneys, lungs, digestive system, eyes, skin, nervous system and other extra-articular organs.[2,3] The cause of RA is unknown, it is mainly related to the genetics, environment, and autoimmunity.[4,5]

Clinical anti-RA drugs are divided into symptomatic treatment and disease modifying management. Symptomatic treatment including nonsteroidal anti-inflammatory drugs (NSAIDs) and glucocorticoids (GCs), whose goal is to reduce inflammation and pain, while disease modifying drugs are mainly DMARDs, which aim to improve cartilage injury and joint deformity.[6,7] However, adverse effects and side effects can occur with the long-term use of GCs, NSAIDs, and

Received: 6 September 2022
Accepted: 2 February 2023
Published: 11 February 2023

DMARDs, such as gastrointestinal bleeding, hepatorenal toxicity, cardiovascular disease, and stomatitis,[8,9] thus, it is worth exploring effective and safe drugs.

The latest research has revealed that several extracts and active compounds of traditional herbal medicines show potential anti-RA activity, such as flavonoids, phenolic acids, alkaloids, quinones, and triterpenes.[10] Currently, an increasing number of traditional medicines are being applied in clinics, such as Zishen Tongluo formula,[11] Ershiwuwei Lvxue pills,[12] Wenjinghuoluo prescriptions,[13] and Bawei Longzuan granules.[14] *Rubia cordifolia* L. (Rubiaceae, RC) is a sprawling plant, which prefer pleasantly cool and humidity environment and is distributed throughout Greece, Sudan, South-Africa, and Asia.[15] The aqueous leaf extract of RC showed antitumor, DNA-binding, antifungal, and antioxidant properties.[16] While the dry rhizome of RC is recorded in the 2020 edition of the Chinese Pharmacopoeia and are widely used as traditional Chinese medicine for the treatment of tuberculosis, contusions, menoxenia, and rheumatism in China, Japan, Korea, and India.[17] Our previous study indicated that the ethanol extract of *R. cordifolia* (RCE) has significant effects on foot swelling and joint damage.[18] Further investigation found 40 compounds in RCE; 21 compounds were detected in rat plasma and 8 compounds were detected in rat urine after the oral administration of RCE.[19] However, the targets and mechanisms of RCE for treating RA have not been fully clarified.

Metabolomics technology has developed rapidly in recent years. It is defined as a discipline of metabolic analysis at the level of cells or organs. Some studies had disclosed the development of RA were related various metabolism, including glucose metabolism,[20] lipid metabolism,[21] amino acid metabolism,[22] glycerophospholipid metabolism,[23] pyrimidine metabolism,[24] arachidonic acid metabolism[25] and et al. Metabolic disorders and diseases caused by environmental factors, as well as extra-genomic effects such as intestinal flora, are the research objects of metabolomics; the study of related genes, proteins, and biomarkers at the metabolic level will help to uncover the mechanisms of RA.[26,27] The methods for metabolite identification include NMR (nuclear magnetic resonance) spectroscopy, GC–MS (gas chromatography–mass spectrometry), and LC–MS (liquid chromatography–high–resolution mass spectrometry), and the sample for metabolite analysis could be urine or blood serum.[28] In our previous study, RCE showed significant potential anti-RA effects, but the endogenous mechanisms underlying the changes in the metabolites is still unclear. Thus, metabolomics may improve the application of RCE.

Unlike ordinary drugs with single causative genes and individual targets, natural medicine contains many active compounds and can act on two or more targets simultaneously.[29] Network pharmacology is a promising method for exploring and establishing a network of predicted targets and compounds. Therefore, we integrated metabolomics with network pharmacology to determine the key targets and compounds of RCE affecting RA in this study.

The study procedure is shown in Figure 1.

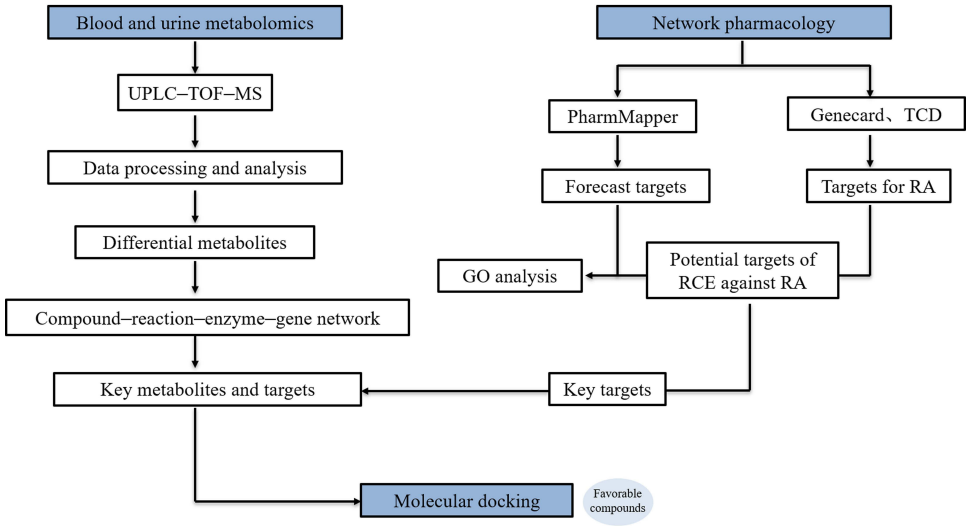

Figure 1 The procedure of the metabolism and network pharmacology experiment.

Materials and Methods

Materials and Reagents

Complete Freund's adjuvant (CFA) was purchased from Sigma–Aldrich (St. Louis, MO, USA); physiological saline was purchased from Guangzhou Litai Pharmaceutical Co., Ltd. (Guangzhou, China); phosphate buffered saline (PBS) was obtained from Gibco (California, USA); paraformaldehyde (4%) was purchased from Ruishu Biotechnology Co., Ltd. (Shanghai, China); and dexamethasone was purchased from Guangdong South China Pharmaceutical Co., Ltd. (Dongguan, China). Mollugin and purpurin (purity: 86.7%) were purchased from the China Biological Products Inspection Institute (Beijing, China); alizarin (purity: 97%) was purchased from Shanghai Aladdin Biochemical Technology Co., Ltd. (Shanghai, China); rubiadin (purity: 98%) was purchased from Shanghai Jingdu Biotechnology Co., Ltd. (Shanghai, China); and 6-hydroxyrubiadin (purity: 97%) was purchased from Shanghai Yunmu Biological Technology Co., Ltd. (Shanghai, China). The TNF-α ELISA kit was purchased from Cusabio Biotech Co., Ltd. (Wuhan, China); IL-1β and prostaglandin (PG)E2 antibodies were purchased from Abcam (Cambridge, UK); and the P65 antibodies and diaminobenzidine (DAB) reagent kit were purchased from Cell Signaling Technology (CST) (Boston, MA, USA).

Plant Materials and Extraction Procedure

Rubia cordifolia L. (batch no. 60863211) was collected from the Chinese Medicine Material Processing Plant of Guangdong Province (Hunan, China) and the dry rhizome were stored at 24 °C and 60% humidity at the Research Center of Chinese Herbal Resource Science and Engineering, Guangzhou University of Traditional Chinese Medicine. The plant was identified by Professor Ruo-Ting Zhan (Guangzhou University of Traditional Chinese Medicine). The extraction process of RC was based on previous study.[18] The reference standards for the amounts of mollugin, purpurin, alizarin, 6-hydroxyrubiadin, and rubiadin were dissolved in ethanol with a concentration of 0.1 mg/mL.

Chemical Composition and Bio-Metabolites Analysis

HPLC Analysis

The chromatographic separation was performed using the Ultimate 3000 HPLC system (Thermo Fisher Scientific, Waltham, MA, USA) equipped with a quaternary pump, diode array detector, autosampler, and a Chromeleon chromatography workstation. The chromatographic column was an Ecosil C18 AQ Plus (4.6 × 250 mm, 5 μm; Knauer, Berlin, Germany). The mobile phase consisted of acetonitrile (eluent A) and 0.1% ammonia trifluoroacetate in water (eluent B; pH was 2.6 with ammonia). The chromatographic separation conditions were as follows: 0–10 min, A: 10–25%, B: 90–75%; 10–23 min, A: 25–35%, B: 75–65%; 23–43 min, A: 35–70%, B: 65–30%; 43–53 min, A: 70%, B: 30%; 53–65 min, A: 70–100%, B: 30–0%; and 65–70 min, A: 100%, B: 0%. The detection wavelength was set at 250 nm, the injection volume was 10 μL, the column temperature was maintained at 35°C, and the flow rate was 1.0 mL/min.

UPLC–Q-TOF/MS Analysis

UPLC–Q-TOF/MS analysis was performed using a Triple TOF 5600 LC/MS/tandem MS system (AB Sciex, Redwood City, CA, USA) coupled to LC-30 AD (Shimadzu, Duisburg, Germany) and 5600 TOF/MS (AB Sciex) systems. The chromatographic column was an ACQUITY ethylene bridged hybrid C18 (100 × 2.1 mm, 1.7 μm; Waters, Milford, CT, USA). The mobile phase consisted of acetonitrile (A) and 0.1% aqueous formic acid (B). The chromatographic separation conditions of the serum were as follows: 0–8 min, A: 95–40%, B: 5–60%; 8–18 min, A: 40–3%, B: 60–97%; and 18–21 min, A: 3%, B:97%. The chromatographic separation conditions of the urine were as follows: 0–2 min, A: 95–92%, B: 5–8%; 2–8 min, A: 92–70%, B: 8–30%; 8–10 min, A: 70–20%, B:30–80%; 10–11 min, A: 20%, B: 80%; 11–12 min, A: 0%, B:100%; and 12–13 min, A: 0%, B: 100%. The sample injection volume was 2 μL, the column temperature was maintained at 35 °C, and the flow rate was 0.3 mL/min. The data were simultaneously collected in positive and negative ion modes (electrospray ionization ESI+ and ESI− modes, respectively) with a scan range (m/z) of 100–1000. The optimized parameters for ESI+ were as follows: gas temperature, 600 °C; nebulizer gas pressure, 55 psi; ion spray voltage floating, 5.5 kV; and collision energy, 10 V. The optimized parameters for ESI− were as follows: gas temperature, 500 °C; nebulizer gas pressure, 55 psi; ion spray voltage floating, 4.5 kV; and collision energy, 10 V. Quality control samples were used to monitor sample stability during the experiment.

Animal Experiment

Animal Feeding Conditions

72 adult male Wistar rats (certificate number: SCXK Yue 2016–0041, animal ethics approval number: 20160401002, weighing 180–220 g) were obtained from the Experimental Animal Center of Southern Medical University and housed under controlled conditions at 20–25 °C and a relative humidity of 40–60%, on a 12:12 h light/dark cycle with free access to food and water.

AIA Model Establishment and Drug Treatment

After adaptive feeding, the rats were randomly allocated to six groups (n = 12 per group), including the control group, the AIA group, the AIA + RCE high-dose group, the AIA + RCE medium-dose group, the AIA + RCE low-dose group, and the AIA + Dex group (standard control group). All groups, except the control group, were subcutaneously injected in the right hind paw with 0.1 mL CFA, and the control group was injected with an equivalent volume of physiological saline. After 14 days, the treatment groups were treated with RCE[18] (high-dose group: 10 g/kg, medium-dose group: 5 g/kg, and low-dose group: 2.5 g/kg) and Dex (0.125 mg/kg), and the control group was given the same volume of distilled water for 21 days.

During modeling and administration, the body weight and foot swelling of the rats were recorded once every 3 days. The paw swelling was measured by the volumetric method. The weight gain rate was calculated with the following formula: growth rate (%) = (Mt−M0)/M0, where M0 and Mt are weight on the day of RCE administration (day 0) and on day t after administration, respectively.

Biological Sample Processing

The blood and urine samples of the rats were collected at 0, 7, 14, and 21 days after RCE administration. The samples were centrifuged at 1500g for 10 min at 4 °C, and the supernatant was collected and stored at −80 °C. Proteins in 100 μL of serum or urine were removed by dissolving in methanol, followed by vortexing for 60s and incubation at 4 °C for 30 min, after which they were centrifuged at 1500g for 15 min at 4 °C. The supernatant was vacuum dried at 37 °C, and the pellet was reconstituted in 200 μL methanol. The pooled quality control (QC) samples were composed of 10 μL aliquots from each sample.

Hematologic Analysis (HE), Immunocytochemistry (IHC) and Enzyme Linked Immunosorbent Assay (ELISA)

Twenty-eight days after RCE administration, the joints of the rats were immersed in 4% buffered formaldehyde fixative. We prepared paraffin-embedded sections (5 μm) and stained them with hematoxylin and eosin.[30]

The expressions of IL-1β, PGE2, and P65 in the joints were detected by immunocytochemistry (IHC). Paraffin sections were dewaxed, repaired with citric acid, incubated with 3% hydrogen peroxide, washed by PBS, and blocked with goat serum. Then, the sections were incubated with primary antibodies for 2 h at room temperature, washed with PBS, incubated with biotinylated secondary antibodies, washed, and incubated with horseradish peroxidase and streptavidin. Finally, DAB was used for color development.[31] The expression of IL-1β, PGE2, and P65 was detected using image pro plus6.0 image analysis software and was presented using optical density (OD) values.

The joints of the rats were homogenized in saline solution and centrifuged with 1500g at 4 °C for 15min. The supernatant was detected according to the ELISA kit's protocol, added the sample and incubated for 2 h at 37 °C, then added biotin antibody (1x) and incubated for 1 h at 37 °C, then added HRP avidin (1x) to each well after washed, incubated for 1 h at 37 °C, then added chromogenic substrate and incubated for 15–30 minutes at 37 °C with protected from light, finally stop solution was added and measured at 450 nm.[32]

Data Analysis

The UPLC/MS raw data were preprocessed by Peak View Shortcut software (AB Sciex). Then, they were imported into SIMCA P 14.0 (Sartorius, Göttingen, Germany) software for principal component analysis (PCA) and orthogonal partial least squares discriminant analysis (OPLS-DA). A score plot was used to visualize differences between groups. The variable importance in projection (VIP) value (VIP > 1) and a *t*-test ($p < 0.05$) were used to screen potential biomarkers of RA.[33] Based on the molecular weight and fragmentation patterns in the mass spectra, the compounds were identified using METLIN (a powerful database for metabolite identification and query, Scripps Research, La Jolla, CA, USA; http://metlin.scripps.edu) and the Human Metabolome Database (HMDB, a database containing detailed information on

human small molecule metabolites; http://www.hmdb.ca). The detected metabolites were analyzed using the MetaboAnalyst (http://www.MetaboAnalyst.ca/), Kyoto Encyclopedia of Genes and Genomes pathway (http://www.genome.jp/eg), HMDB, and METLIN databases.

Network Pharmacology Construction

The compounds of RCE were collected according to a previous study,[19] the forecast targets of compounds were obtained from the Traditional Chinese Medicine Systems Pharmacology Database and Analysis Platform (TCMSP, a unique systems pharmacology platform of Chinese herbal medicines that captures the relationships between drugs, targets and diseases, https://old.tcmsp-e.com/tcmsp.php) and PharmMapper databases (an online platform for pharmacophore matching and potential target identification, http://lilab-ecust.cn/pharmmapper/index.html); the disease targets were collected from the GeneCards (https://www.genecards.org/) and Comparative Toxicogenomics database (CTD, a database for studying the relationships among chemicals, genes, phenotypes, diseases and environments, https://ctdbase.com/) with the keyword "rheumatoid arthritis". The protein–protein interaction (PPI) network was established by the STRING platform (https://cn.string-db.org/), and Cytoscape 3.5.0 software (National Institute of General Medical Sciences, USA) was used to explore the potential targets of RCE to treat RA by screening the coincident targets of the forecast targets and RA targets. The potential targets were analyzed by the network analysis function, and the Gene Ontology (GO) enrichment pathway was analyzed by GluGo (a plugin with enrichment functions). The differential metabolites were imported into the Metascape plugin for Cytoscape 3.5.0 software, and we constructed a compound–enzyme–reaction–gene network. The key targets and compounds were obtained by analyzing the integration of potential targets and the metabolite network analysis.[34–36]

Molecule Docking

The crystal structures of targets including CLC (PDB ID: 6GKT), PLA2G2A (PDB ID: 1DB5), CDA (PDB ID: 1JTK), PLA2G10 (PDB ID: 6G5J), NT5M (PDB ID: 1Q92) and UCK2 (PDB ID: 1UDW) were acquired from PDB database (https://www.rcsb.org/). The structure of the RCE components was obtained from the PubChem database (https://pubchem.ncbi.nlm.nih.gov/) and converted to PDB format using Open Babel software. The targets and components of RCE were converted to pdbqt format using AutoDockTools 1.5.6 software (software to perform ligand-protein molecular docking, Scripps Institute, USA). Then, the water molecules were deleted from the structures, and we added hydrogen atoms and charged the gasteiger. The docking boxes are listed in Table S1, with size_x = 40, size_y = 40, and size_z = 40 for each target. The docking run option parameters were set to default values. Finally, the docking results with the highest scores were visualized by PyMoL software.[37]

Statistical Analysis

The data were analyzed by statistical product service solutions (SPSS) v19.0 software and are expressed as the mean ± standard deviation (SD). The data were normally distributed with uniform variance. One-way analysis of variance was used for comparisons between groups; for other statistical analyses, the Log rank test was used, and p values of ≤ 0.05 were considered statistically significant.

Results

RCE Treatment Improved Symptoms in AIA Rats

The components of RCE were confirmed before treatment; alizarin, 6-hydroxyrubiadin, purprin, rubiadin, and mollugin were identified in this study (Figure 2), and the standards and purity of the definitive components exceeded 95% (Figures S1 and S2).

As shown in Figure 3A, RCE administration had little effect on the weight of the rats; however, due to the side effect of GCs, the growth rate of the rats was slow with Dex treatment.[38] During the dosing period, the inhibition of foot swelling by Dex was remarkable, and RCE also showed significant inhibition of foot swelling and improved the redness of AIA rats (Figure 3B and C). Histological sections of the joints showed similar improvements after the RCE intervention; in the AIA group, the articular cartilage had defects (black arrow), the synovial cells had increase (red arrow), and the inflammatory cells were infiltrated (yellow arrow) in the joints of the rats. With the treatment of RCE, especially in the high-dose group, the surface of the articular cavity became smooth and there was almost no inflammatory cell infiltration (Figure 3D).

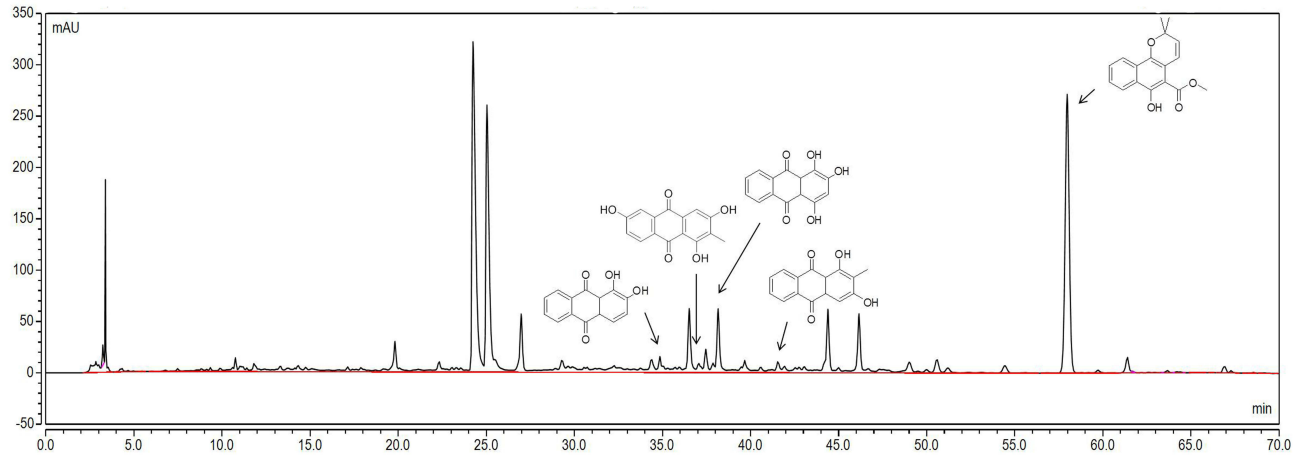

Figure 2 Identification of components in RCE based on HPLC. The chemical composition, from left to right, is alizarin, 6-hydroxyrubiadin, purpurin, rubiadin, and mollugin. **Abbreviations**: RCE, ethanol extract of *Rubia cordifolia* L.

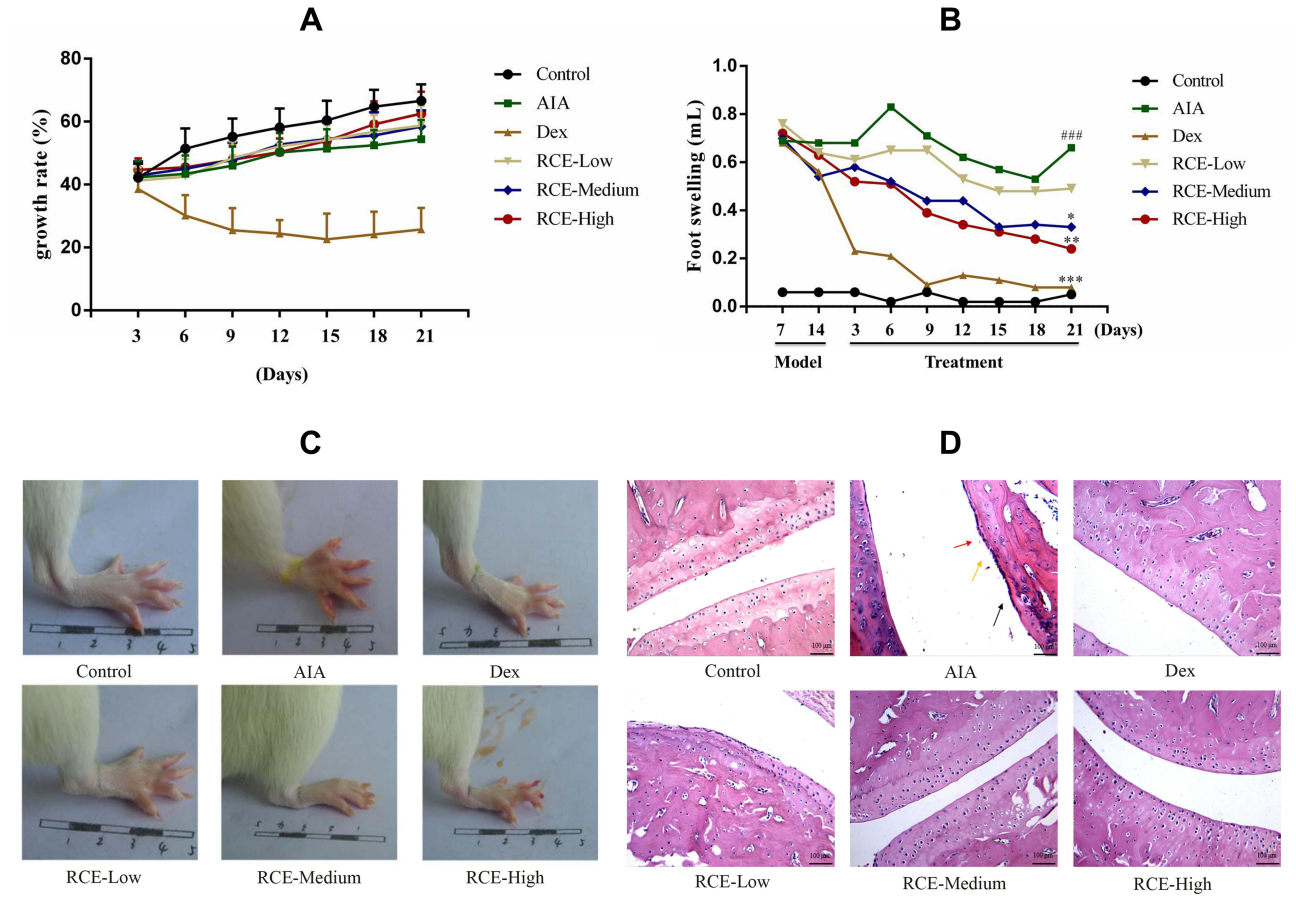

Figure 3 Therapeutic effects of RCE on AIA rats. RCE was orally administered once daily for 21 days. (**A**) Changes in the weight of rats during administration. (**B**) Attenuation of foot swelling in AIA rats treated with RCE. (**C**) The appearance of the feet; the image was collected on day 21 after RCE administration. (**D**) HE staining of rat joints (magnification: 100 folds). The joints images were collected on day 21 after RCE administration. Articular cartilage injury (black arrow), membranous cell fibrosis (red arrow), inflammatory cell infiltration (yellow arrow). Data are presented as the mean ± SD. $^{###}p < 0.001$ vs control. $^{***}p < 0.001$, $^{**}p < 0.01$, $^{*}p < 0.05$ vs model, n = 8. **Abbreviations**: RCE, ethanol extract of *Rubia cordifolia* L.; Control, control group; AIA, AIA model group; Dex, dexamethasone group; RCE—Low; RCE low-dose group; RCE—medium; RCE medium-dose group; RCE—High; RCE high-dose group.

In order to confirm the anti-inflammatory effect of RCE, the levels of TNF-α, IL-1β, PGE2, and P65 were detected in this experiment. In the AIA group, the levels of TNF-α, IL-1β, PGE2, and P65 were obviously increased. However, the contents of TNF-α, IL-1β, PGE2, and P65 were decreased by RCE treatment (Figure 4).

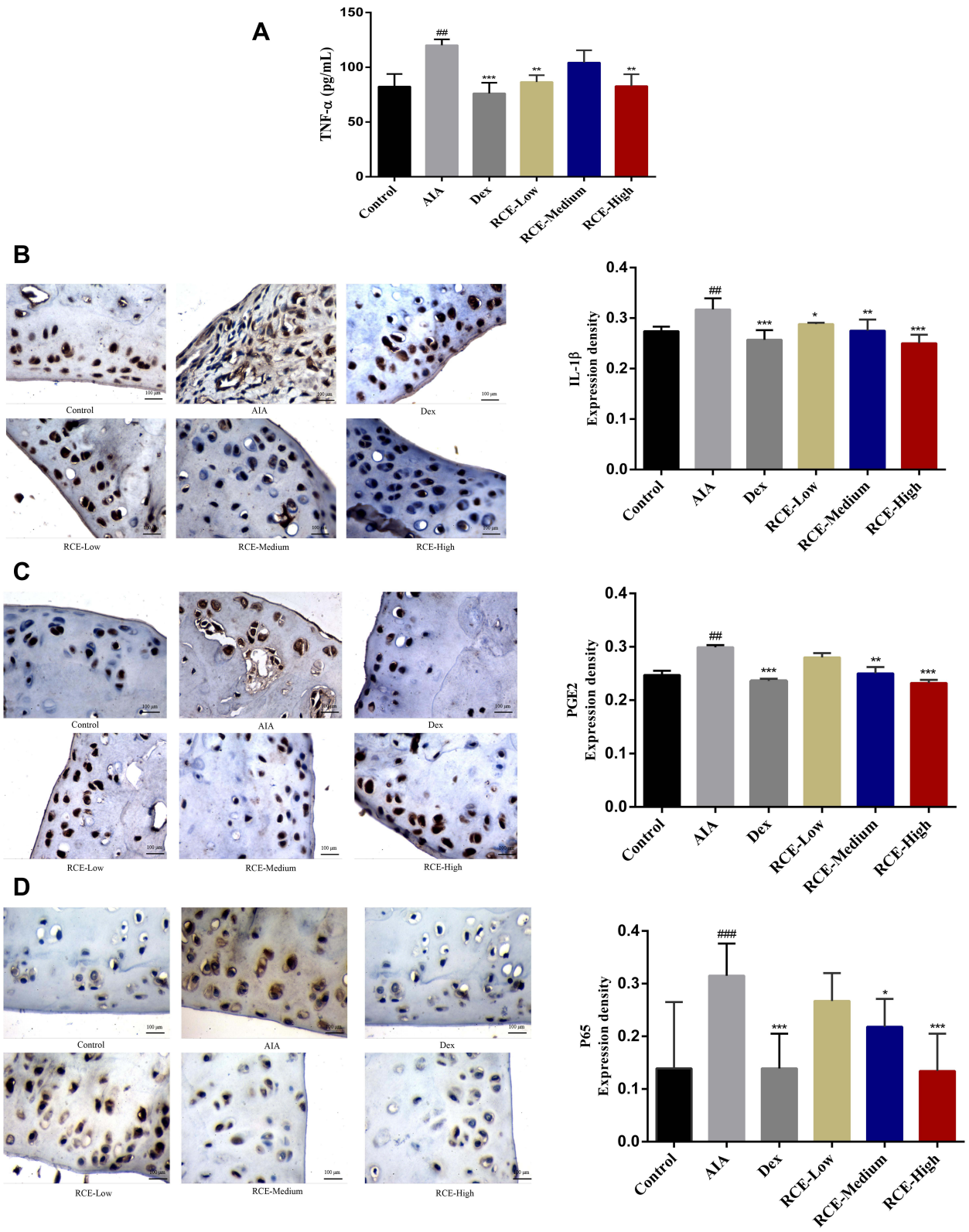

Figure 4 The anti-inflammatory effect of RCE in AIA rats. (**A**) The inhibitory effect of RCE on TNF-α. (**B**) The inhibitory effect of RCE on IL-1β. (**C**) The inhibitory effect of RCE on PGE2. (**D**) The inhibitory effect of RCE on P65. The expression of TNF-α was detected by ELISA. IL-1β, PGE2, and P65 were detected by IHC, magnification: 100 folds. Data are presented as the mean ± SD. $^{###}p < 0.001$, $^{##}p < 0.05$ vs control. $^{***}p < 0.001$, $^{**}p < 0.01$, $^{*}p < 0.05$ vs model, n = 8.
Abbreviations: TNF-α, tumor necrosis factor α; IL-1β, Interleukin-1β; PGE2, prostaglandin E2; IHC, immunocytochemistry.

Metabolomics Profiling

Changes in the serum metabolite composition in the rats at 7, 14, and 21 days were analyzed by OPLS–DA; the representative total ion chromatograms (TICs) of the ionization modes are shown in Figure S3. On day 7, the cluster of RCE and AIA groups were close to each other, but there were significant differences with the control group. Over time, the cluster of RCE group was distinct from the AIA group, and the condition was more obvious at 21 days post administration, indicating that RCE reversed the metabolic disorder observed in the AIA model (Figure 5A).

Changes in the urine metabolites of the rats were also assessed at 7, 14, and 21 days; the representative TICs of the ionization modes are shown in Figure S4. The metabolite profiles of the RCE treatment groups differed significantly from those of the AIA group, while the effects of RCE had a slow onset compared with Dex (Figure 5B). The presentive TICs showed that QC samples behaved stably during the experiment (Figures S5 and S6).

Differential Metabolite Identification and Pathway Analysis

The ten differential metabolites in the serum of the rats were 5-hydroxyindoleacetic acid, lysoPE(0:0/22:1(13Z)), tetracosahexaenoic acid, mevalonic acid-5P, linoleyl carnitine, LysoPC (20:2 (11Z,14Z)), allopregnanolone, palmitic amide, (R)-3-hydroxy-hexadecanoic acid, and oleic acid. These metabolites are related to tryptophan metabolism, glycerophospholipid metabolism, glucuronidation metabolism, terpenoid backbone biosynthesis, fatty acid metabolism, and the biosynthesis of un-saturated fatty acids (Table 1).

Seven differential metabolites were identified in the urine of the rats, ie, 13-Oxo-9,11-tridecadienoic acid, phenyllactic acid, cytidine, prolylhydroxyproline, phenylacetylglycine, acetylcysteine, and indoleacetic acid. These are related to phenyl-alanine metabolism, pyrimidine metabolism, proline metabolism, oxidative damage, and tryptophan metabolism (Table 2).

Finally, the metabolites detected in the serum and urine after RCE treatment were involved in six pathways, namely, steroid biosynthesis ($p = 0.17204$), tryptophan metabolism ($p = 0.01473$), glycerophospholipid catabolism ($p = 0.04444$), and pyrimidine metabolism ($p = 0.00709$), which are closely related the metabolism of rats (Figure 5C).

Network Pharmacology

According to our previous study, nine compounds were collected for network pharmacology analysis, including munjistin, 6-Hydroxyrubiadin, alizarin, purpurin, ruberythric acid, rubiadin, pseudopurpurin, physcion, and nordamnacanthal (Table 3). A total of 270 forecast targets of compounds also were collected from the PharmMapper database. A total of 2000 targets of RA were obtained from the GeneCards and CTD databases. The "compounds–forecast targets–RA targets" network was constructed and analyzed by Cytoscape software; potential targets were the coincidence targets of both forecast targets and RA targets (Figure 6A).

To uncover the biological function of the potential targets, we performed GO analysis by the GlueGO plugin for Cytoscape software (Figure 6B). The top terms of the GO analysis were leukocyte activation, regulation of kinase activity, and positive regulation of cell population proliferation.

Integrated Analysis of Metabolomics and Network Pharmacology

The differential metabolites were imported into the MetScape plugin for Cytoscape software to obtain the compound–reaction–enzyme–gene network. We found six key targets (genes) that matched the potential targets in network pharmacology, ie, CLC, PLA2G2A, CDA, PLA2G10, NT5M, and UCK2 (Table 4). The key related metabolites were LysoPC (20:2 (11Z,14Z)) and cytidine. The related metabolic pathways were glycerophospholipid metabolism and pyrimidine metabolism (Figure 6C).

Molecular Docking

The ΔG binding energy of the related compounds and key targets is shown in Table S2, the compound with the lowest binding energy was named the favorable compound of target.

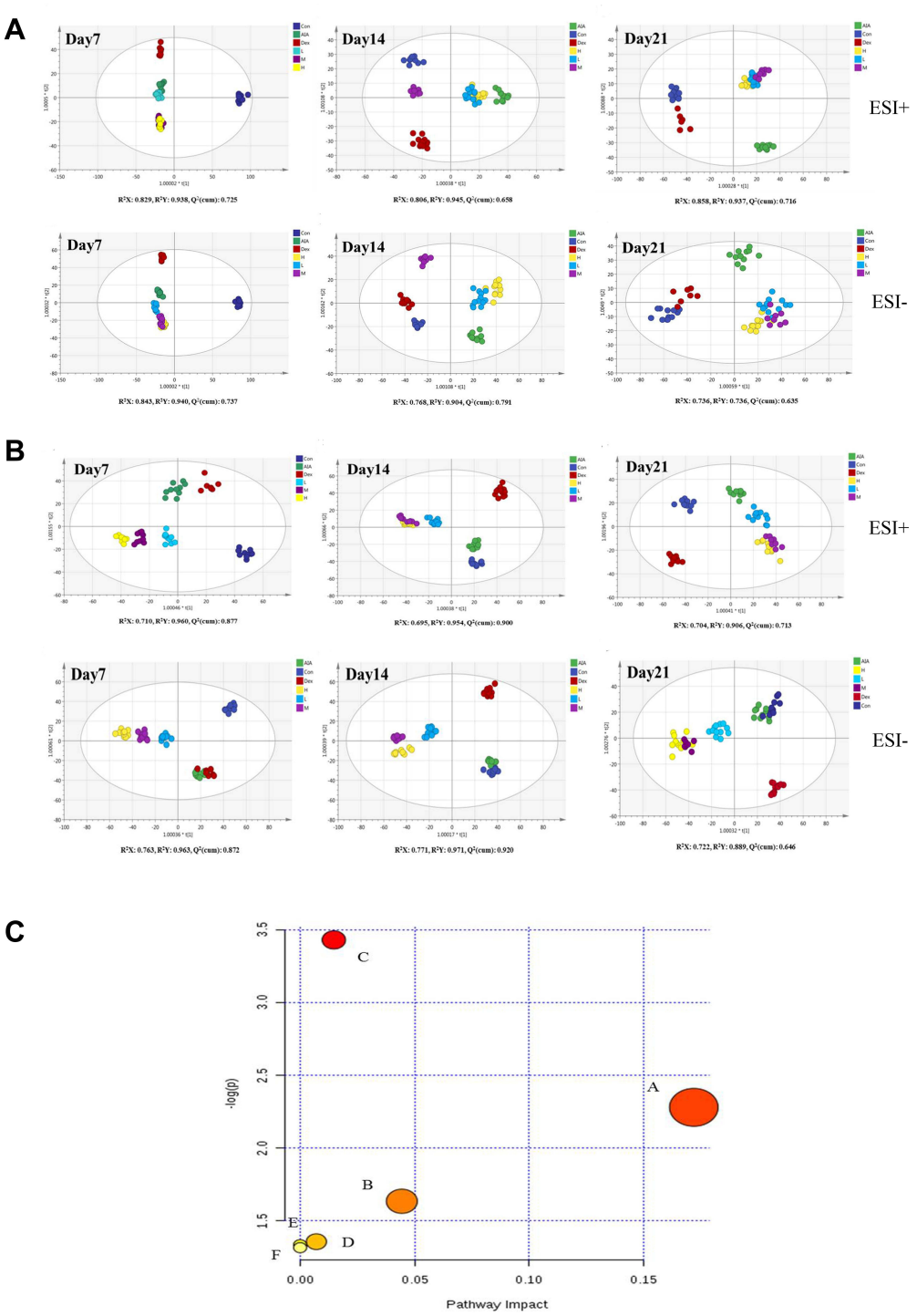

Figure 5 The metabolite profiles changes and pathway enrichment in the serum and urine of the rats. (**A**). The metabolite changes in the serum at 7, 14, and 21 days of treatment. ESI+ mode: R2X = 0.829, R2Y = 0.938, and Q2 (cum) = 0.725 on day 7; R2X = 0.806, R2Y = 0.945, and Q2 (cum) = 0.658 on day 14; and R2X = 0.858, R2Y = 0.937, and Q2 (cum) = 0.716 on day 21. ESI− mode: R2X = 0.843, R2Y = 0.940, and Q2 (cum) = 0.737 on day 7; R2X = 0.768, R2Y = 0.904, and Q2 (cum) = 0.791 on 14 day; and R2X = 0.736, R2Y = 0.851, and Q2 (cum) = 0.635 on day 21. (**B**). The metabolite changes in the urine at 7, 14, and 21 days of treatment. ESI+ mode: R2X = 0.710, R2Y = 0.960, and Q2 (cum) = 0.877 on day 7; R2X = 0.695, R2Y = 0.954, and Q2 (cum) = 0.900 on day 14; and R2X = 0.704, R2Y = 0.906, and Q2 (cum) = 0.713 on day 21. ESI− mode: R2X = 0.763, R2Y = 0.963, and Q2 (cum) = 0.872 on day 7; R2X = 0.771, R2Y = 0.971, and Q2 (cum) = 0.920 on day 14; and R2X = 0.722, R2Y = 0.889, and Q2 (cum) = 0.646 on day 21. Control group (dark blue), AIA group (green), Dex group (red), RCE high-dose group (yellow), RCE medium-dose group (purple), and RCE low-dose group (light blue). (**C**) Pathway enrichment of serum and urine metabolites. (A) Steroid biosynthesis, p = 0.17204. (B) Glycerophospholipid metabolism, p = 0.04444. (C) Tryptophan metabolism, p = 0.01473. (D) Pyrimidine metabolism, p = 0.00709. (E) Biosynthesis of unsaturated fatty acids. (F) Fatty acid biosynthesis.

https://doi.org/10.2147/DDDT.S388932 DovePress

Table 1 Metabolites in the Serum of Rats

Metabolite	Formula	RT (min)	Measured m/z	Theoretical m/z	Error (ppm)	VIP	Trend	ESI Mode	HMDB ID	Metabolic Pathway
5-Hydroxyindoleacetic acid	$C_{10}H_9NO_3$	2.16	192.06554	192.06552	0.1	1.490	↓*	+	0060400	A
LysoPE (0:0/22:1 [13Z])	$C_{27}H_{52}NO_7P$	4.65	534.34858	534.35542	−6	1.307	↓**	+	0011491	B
Tetracosahexaenoic acid	$C_{24}H_{36}O_2$	8.22	357.27902	357.27881	0.3	1.745	↓**	+	02007	C
Mevalonic acid-5P	$C_6H_{13}O_7P$	10.59	229.04717	229.04886	7.4	1.786	↓*	+	0001343	D
Linoleyl carnitine	$C_{25}H_{45}NO_4$	11.16	424.34205	424.34214	−0.2	2.072	↓*	+	0006469	E
LysoPC (20:2 (11Z,14Z))	$C_{28}H_{54}NO_7P$	12.47	548.37105	548.37107	0	1.235	↓**	+	0010392	B
Allopregnanolone	$C_{21}H_{34}O_2$	17.99	319.26313	319.26316	−0.1	1.550	↓**	+	0006759	E
Palmitic amide	$C_{16}H_{33}NO$	18.04	256.26373	256.26349	0.9	1.323	↑**	+	0012273	U
(R)-3-Hydroxy-hexadecanoic acid	$C_{16}H_{32}O_3$	14.78	271.22810	271.22787	0.9	1.110	↓*	−	0010734	E
Oleic acid	$C_{18}H_{34}O_2$	17.39	281.24857	281.24860	−0.1	1.306	↓*	−	0000207	F

Notes: A, tryptophan metabolism; B, glycerophospholipid metabolism; C, glucuronidation metabolism; D, steroid biosynthesis; E, fatty acid metabolism; ESI, electrospray ionization; F, biosynthesis of unsaturated fatty acids; ↑, uptrend of RCE group relative to model group; ↓, downward of RCE group relative to the model group, *P<0.05, **P<0.01 vs model.

Abbreviations: HMDB ID, Human Metabolome Database identification number; LysoPC, lysophosphatidylcholine; LysoPE, lysophosphatidylethanolamine; RT, retention time; U, unknown; VIP, variable importance in projection.

Table 2 Metabolites in the Urine of Rats

Metabolite	Formula	RT (min)	Measured m/z	Theoretical m/z	Error (ppm)	VIP	Trend	ESI Mode	HMDB ID	Metabolic Pathway
13-Oxo-9,11-tridecadienoic acid	$C_{13}H_20O_3$	5.96	225.14814	225.14852	−1.7	1.294	↑**	+	0034564	U
Phenyllactic acid	$C_9H_{10}O_3$	6.5	167.06999	167.07027	−1.7	1.379	↑*	+	0000779	A
Cytidine	$C_9H_{13}N_3O_5$	7.97	244.09182	244.0928	−4	1.076	↓**	+	0000089	B
Prolylhydroxyproline	$C_{10}H_{16}N_2O_4$	4.34	227.10371	227.10373	−0.1	1.498	↓*	−	0006695	C
Phenylacetylglycine	$C_{10}H_{11}NO_3$	5.9	192.06664	192.06662	0.1	1.205	↓**	−	0000821	A
Acetylcysteine	C_8HNO_3	7.08	162.03532	162.03532	0	1.124	↓**	−	0001890	D
Indoleacetic acid	$C_{10}H_9NO_2$	8.35	174.05603	174.05605	−0.1	1.090	↓*	−	0000197	E

Notes: A, tryptophan metabolism; B, glycerophospholipid metabolism; C, glucuronidation metabolism; D, steroid biosynthesis; E, fatty acid metabolism; ESI, electrospray ionization; F, biosynthesis of unsaturated fatty acids; ↑, uptrend of RCE group relative to model group; ↓, downward of RCE group relative to the model group, *P<0.05, **P<0.01 vs model.

Abbreviations: HMDB ID, Human Metabolome Database identification number; RT, retention time; U, unknown; VIP, variable importance in projection.

https://doi.org/10.2147/DDDT.S388932

Table 3 Compounds in RCE for Network Analysis

Name	PubChem CID	Canonical SMILES
Munjistin	160,476	C1=CC=C2C(=C1)C(=O)C3=CC(=C(C(=C3C2=O)O)O)C(=O)O)O
6-Hydroxyrubiadin	5,319,801	CC1=C(C=C2C(=C1O)C(=O)C3=C(C2=O)C=C(C=C3)O)O
Alizarin	6293	C1=CC=C2C(=C1)C(=O)C3=C(C2=O)C(=C(C=C3)O)O
Purpurin	6683	C1=CC=C2C(=C1)C(=O)C3=C(C2=O)C(=C(C=C3O)O)O
Ruberythric acid	92,101	C1C(C(C(C(O1)OCC2C(C(C(C(O2)OC3=C(C4=C(C=C3)C(=O)C5=CC=CC=C5C4=O)O)O)O)O)O)O)O)O
Rubiadin	124,062	CC1=C(C=C2C(=C1O)C(=O)C3=CC=CC=C3C2=O)O
Pseudopurpurin	442,765	C1=CC=C2C(=C1)C(=O)C3=C(C2=O)C(=C(C(=C3O)C(=O)O)O)O
Physcion	10,639	CC1=CC2=C(C(=C1)O)C(=O)C3=C(C2=O)C=C(C=C3O)OC
Nordamnacanthal	160,712	C1=CC=C2C(=C1)C(=O)C3=CC(=C(C(=C3C2=O)O)O)C=O)O

The docking analysis of PLA2G2A showed that alizarin formed hydrogen bonds with HIS-47 and ASP-48 at active sites, the binding energy was −7.53 kcal/mol (Figure 7A, Table S2). The docking analysis of PLA2G10 showed that 6-hydroxyrubiadin formed hydrogen bonds with GLY-30, ASP-47, HIS-46, and PRO-17 and the binding energy was −8.29 kcal/mol (Figure 7B, Table S2)). The docking analysis of CLC showed that ruberythric acid formed hydrogen bonds with the targets; the related residues were GLU-46, GLN-125, PRO-7, and THR-9, the binding energy was −5.58 kcal/mol (Figure 7C, Table S2). The docking analysis of UCK2 showed that munjistin interacted with targets with ALA-30, LYS-33, ARG-166, ASP-84, ARG-175, and TYR-65, the binding energy was −7.19 kcal/mol (Figure 7D, Table S2). The docking analysis of CDA showed that 6-hydroxyrubiadin formed hydrogen bonds with GLU-44, GLU-55, ALA-54, and ASN-4, the binding energy was −7.4 kcal/mol (Figure 7E, Table S2). The docking analysis of NT5M showed that 6-hydroxyrubiadin formed hydrogen bonds with VAL-77, PHE-75, ASP-41, LYS-165, and SER-13 and the binding energy was −8.29 kcal/mol (Figure 7F, Table S2).

Discussion

RA is a type of chronic autoimmune disease characterized by redness, swelling, and heat and pain in the joints. The etiology and pathogenesis of RA are diverse and complex. Scientists have reported that the pathogenesis of RA may interact with genetic, epigenetic, environmental, metabolic, immune, and microbial factors.[39,40]

An appropriate animal model is useful for research on complicated systems such as RA involving inflammation, immunity, and metabolism. The AIA rat model was established by CFA induction with a rapid onset and has wide reproducibility. The clinical features of AIA rats, such as joint swelling, synovial infiltration, and cartilage degradation, are similar to those seen in human RA disease; thus, AIA rat model is widely used in research to investigate the pathogenesis of RA.[41,42] In this study, foot swelling and redness were observed in the AIA rats; however, RCE significantly reduced foot swelling and alleviated joint damage (Figure 2).

It is well known that the progression of RA involves the perplexing interaction of inflammation. The proinflammatory cytokines TNF-α and IL-1β are the primary factors inducing inflammation in RA, and they are secreted by synovial fibroblasts and activated macrophages.[43,44] TNF is overexpressed in RA patients, and scientists are becoming aware of the importance of TNF, especially TNF-α.[45] RA treatment has been revolutionized with the advent of TNF-α inhibitors, such as infliximab,[46] adalimumab,[47] and golimumab.[48] The secretion of TNF-α can also promote the synthesis and secretion of IL-1β, which is a positive feedback regulator.[49] IL-1β activates monocytes/macrophages, thus leading to increased inflammation. It also induces the proliferation of fibroblasts and activates chondrocytes and osteoclasts, leading to the deterioration of RA.[50] NF-κB signaling plays a crucial role in the development of RA. IL-1β and TNF-α stimulate P65/P50, causing accumulation at the active site.[51] P65 is an important member of the NF-κB family, when the NF-κB

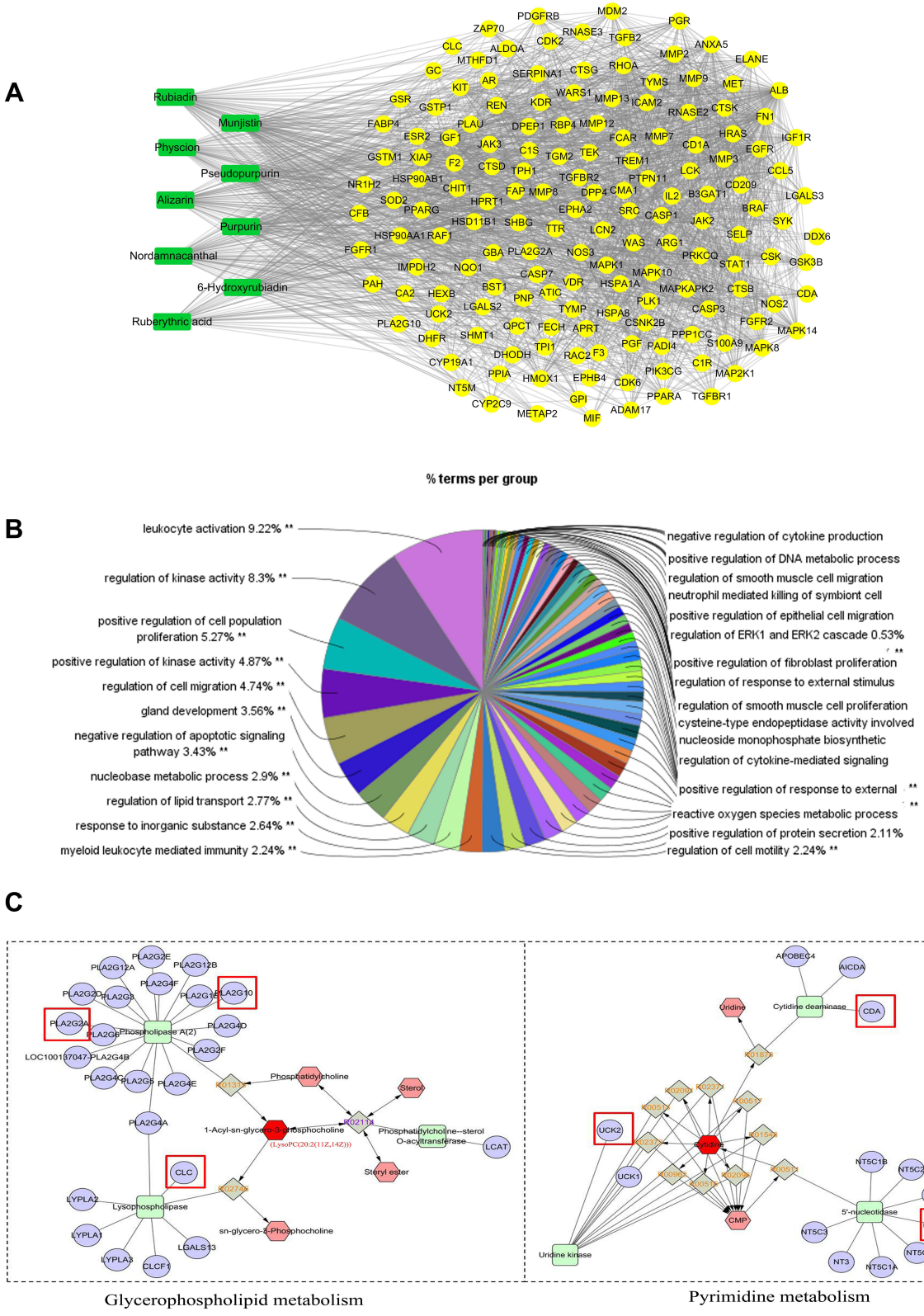

Figure 6 The network pharmacology construction and analysis. (**A**) The active potential targets of RCE for the treatment of RA. (**B**) The GO enrichment analysis of potential targets. The significant level was 0.05, $^{**}p < 0.01$. (**C**) The compound–reaction–enzyme–gene networks of glycerophospholipid metabolism and pyrimidine metabolism. The key targets are marked with a red square. The KEGG ID was same of 1-Acyl-sn-glycero-3-phosphocholine and LysoPC (20:2 (11Z,14Z)), LysoPC (20:2 (11Z,14Z)) is showed as 1-Acyl-sn-glycero-3-phosphocholine in MetScape. Green square: enzyme, purple circle: target, red hexagon: input, gray diamond: reaction, pink hexagon: compound.

https://doi.org/10.2147/DDDT.S388932 DovePress

Table 4 The Information of Metabolism Pathway, Key Targets, and Active Compounds

Related Pathway	Key Targets	Metabolites	KEGG ID
Glycerophospholipid metabolism	PLA2G2A, PLA2G10, CLC	LysoPC (20:2 (11Z,14Z))	C04230
Pyrimidine metabolism	UCK2, CDA, NT5M	Cytidine	C00475

inhibitor α (IκBα) is activated, P65 translocates into the nucleus and an increased content of P65 leads to the activation of a series of inflammatory and immune disorders; thus, the NF-κB P65 signaling pathway is worth paying attention to for drug discovery.[52,53] PGE2, a member of the prostate family with both anti-inflammatory and inflammatory effects, oversecretes IL-1β, resulting in high levels of PGE2, which is also a major target of RA treatment.[54] In this study, we

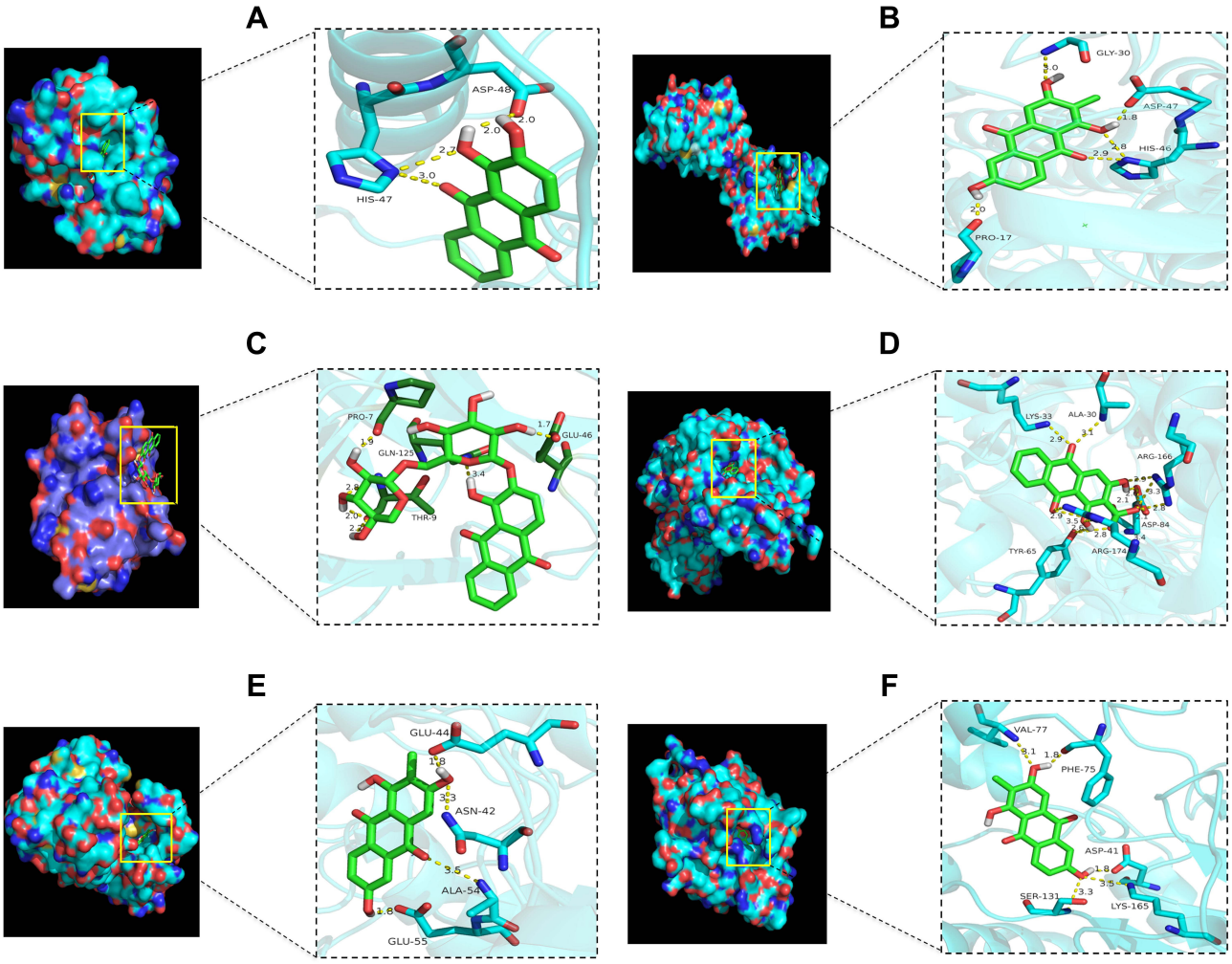

Figure 7 The 3D interaction diagrams of the active compounds and key targets. (**A**) The interaction of PLA2G2A and alizarin, the interacting amino acids were ASP 48 (bond length: 2.0 Å, 2.0 Å) and HIS-47 (bond length: 2.7 Å, 3.0 Å). (**B**) The interaction of PLA2G10 and 6-hydroxyrubiadin, the interacting amino acids were GLY-30 (bond length: 3.0 Å), ASP-47 (bond length: 1.8 Å), HIS-46 (bond length: 2.8 Å, 2.9 Å), and PRO-17 (bond length: 2.0 Å). (**C**) The interaction of CLC and ruberythric acid, the interacting amino acids were PRO-7 (bond length: 1.9 Å), THR-9 (bond length: 2.8, 2.0 and 2.2 Å, respectively), GLN-125 (bond length: 3.4 Å), and GLU-46 (bond length: 1.7 Å). (**D**) The interaction of UCK2 and munjistin, the interacting amino acids were LYS-33 (bond length: 2.9 Å), ALA-30 (bond length: 3.1 Å), ARG-166 (bond length: 2.9, 3.3 and 2.8 Å), ASP-84 (bond length: 2.1, 2.1 and 2.6 Å, respectively), TRY-65 (bond length: 2.6 Å, 2.8 Å), and ARG-174 (bond length: 2.9 Å, 3.5 Å). (**E**) The interaction of CDA and 6-hydroxyrubiadin, the interacting amino acids were GLU-44 (bond length: 1.8 Å), ASN-42 (bond length: 3.3 Å), ALA-54 (bond length: 3.5 Å), and GLU-55 (bond length: 1.8 Å). (**F**) The interaction of NT5M and 6-hydroxyrubiadin, the interacting amino acids were VAL-77 (bond length: 3.1 Å), PHE-75 (bond length: 1.8 Å), SER-131 (bond length: 3.3 Å), LYS-165 (bond length: 3.5 Å), and ASP-41(bond length: 1.8 Å).

Abbreviations: PLA2G2A, phospholipase A2 group IIA; PLA2G10, phospholipase A2 group X; CDA, cytidine deaminase; UCK2, uridine-cytidine kinase 2; CLC, charcot-lLeyden crystal galectin; NT5M, 5′,3′-nucleotidase, mitochondrial.

demonstrated that the expressions of TNF-α, IL-1β, P65, and PGE2 were reduced after treatment with RCE, indicating that RCE may have anti-inflammatory properties and may improve joint damage through the inhibition of these factors. However, regarding the intricate interaction between cytokines and enzymes, we are not sure of the direct effect of RCE on TNF-α, IL-1β, P65, and PGE2; the exact mechanism should be further explored in future studies.

By combing metabolite analysis and network pharmacology, we found six key targets (PLA2G2A, PLA2G10, CLC, UCK2, CDA, and NT5M) and related metabolites, including LysoPC (20:2 (11Z,14Z)) and cytidine, in the glycerophospholipid and pyrimidine metabolism pathways; four favorable compounds (alizarin, 6-hydroxyrubiadin, ruberythric acid, and munjistin) of RCE were discovered in this study.

Su et al discovered glycerophospholipid metabolism participates in the pathogenesis of RA by regulating IL-6/JAK signaling pathway.[23] Lyso-pc serves as a chemoattractant of T lymphocytes and is an important component of oxidized low-density lipoprotein (oxLDL).[55] Furthermore, Lyso-pc is involved in many biological processes, such as pro-inflammatory effects, oxidative stress, apoptotic induction, immune regulation, and anti-infective actions.[56] Hegen et al had showed the essential key of PLA2 by PLA2-deficient mice.[57] Under PLA2 catalysis, glycerophospholipid hydrolyzes to lysophospholipid and arachidonic acids. Subsequently, inflammatory mediators were produced by the action of arachidonic acid, such as prostaglandins and leukotrienes, which participated in the inflammatory response.[58] PLA2G2A and PLA2G10 are members of phospholipaseA2 (PLA2). As one of the diagnostic indicators of RA, PLA2G2A is implicated in, and even accelerates, the pathogenesis of RA.[59,60] In another study regarding the mechanism of tripterygium glycosides tablets, the researchers also revealed the effect of PLA2G10 during the treatment of RA.[61] Our study demonstrated that LysoPC (20:2 (11Z,14Z)) interfered AIA through glycerophospholipid metabolism. Molecular docking showed that alizarin and 6-hydroxyrubiadin were closely bound to PLA2G2A and PLA2G10, respectively. (Table S2)Consequently, alizarin and 6-hydroxyalizarin may inhibit the release of inflammatory mediators (TNF-α, IL-1β, P65, and PGE2) by inhibiting the activated PLA2G2A and PLA2G10 in the development of RA. CLC protein, is Galectin-10 protein crystal which form after eosinophils degranulate. CLC is closely related to lysophosphatidases and inhibited lipolytic activity of eosinophil lysophospholipases.[62] Furthermore, CLCs can induce the in vivo expression of IL-1β in patients of eosinophilic disorders.[63] Few studies report the direct relationship between RA and eosinophils, the prevalence of eosinophils in RA patients ranging from 3.2% to 21.6%.[64,65] In future studies, we will design experiments to prove the relationship between ruberythric acid, CLC and IL-1β.

Pyrimidine metabolism delays the initiation and progression of pathologic changes in RA.[66] In our study, the level of cytidine changed with RCE treatment (Table 2). UCK2 is one of the human uridinecytidine kinase genes; it is always classified as a target for the treatment of cancer.[67,68] However, we found munjistin that had favorable binding with UCK2; thus, the effect of UCK2 should be closely considered and verified. In a study of cyclosporine for the treatment of RA, the expression of cytidine deaminase (CDA) in patients can reflect the immunoregulatory effect during therapy.[69] 5′,3′-nucleotidase, mitochondrial (NT5M) is distributed in the mitochondrial matrix and is a 5′-nucleotidase, which may regulate immunity.[70,71] In this study, 6-hydroxyrubiadin was applied to CDA and NT5M simultaneously (Table S2). Whether 6-hydroxyrubiadin and munjistin regulated pyrimidine metabolism through UCK2, CDA and NT5E to alleviate immune disorder and deterioration of RA. Thus, indepth investigations should be carried out to determine the specific effects and mechanisms of the key targets and active compounds. Meanwhile, 6-hydroxyrubiadin, alizarin, ruberythric acid, and munjistin belongs to anthraquinone, the anthraquinone derivatives have a wide range of physiological activities, including anti-inflammatory,[15] antibacterial,[72] antiarthritic.[73] However, the toxicity of anthraquinone derivatives cannot be ignored, several studies had reported that long term use of anthraquinone drugs may lead to diarrhea, colonic melanosis, colonic mucosal melanosis,[74] and even hepatitis.[75,76] Accordingly, the toxicity of 6-hydroxyrubiadin, alizarin, ruberythric acid, and munjistin must be evaluated in further studies.

Conclusion

In conclusion, the use of RCE showed obvious improvements in the foot swelling and joint damage of the AIA rats in our study. Ten and six differential metabolites were found in serum and urine, respectively; they were closely related to six metabolic pathways. The integrated analysis revealed six key targets, as well as related metabolites and pathways, and the interaction between the key targets and potential compounds was validated by molecular docking. Our study provides a foundation for the use of RCE, and its active compounds, such as alizarin, 6-hydroxyrubiadin, ruberythric acid, and

munjistin, may play a key role in metabolism regulation. However, there are some limitations in this study, the key targets focusing on the metabolism and potential compounds of RCE to treat RA still require further studies and verification, and the detection of miRNA regulating transcription factors should be increased to explore the relationship between TNF-α, IL-1β, P65, and PGE2 and key targets.

Abbreviations

RC, *Rubia cordifolia* L.; RCE, ethanol extract of *Rubia cordifolia* L.; RA, rheumatoid arthritis; AIA, adjuvant-induced arthritis; Dex, dexamethasone; TNF-α, tumor necrosis factor-α, IL-1β; interleukin-1β; PGE2, prostaglandin E2; HPLC, High Performance Liquid Chromatography; UPLC, Ultra Performance Liquid Chromatography; HE, hematologic analysis; IHC, immunocytochemistry; TOF, Time-of-flight; CFA, Complete Freund's adjuvant; PBS, phosphate buffered saline; DAB, diamino-benzidine; ELISA, enzyme linked immunosorbent assay; TCMSP, Traditional Chinese Medicine Systems Pharmacology Database and Analysis Platform; CTD, Comparative Toxicogenomics database; PLA2G2A, phospholipase A2 group IIA; PLA2G10, phospholipase A2 group X; CDA, cytidine deaminase; UCK2, uridine-cytidine kinase 2; CLC, charcot-lLeyden crystal galectin; NT5M, 5′,3′-Nucleotidase, Mitochondrial; SPSS, Statistical Product Service Solutions; GCs, glucocorticoids; OPLS–DA, Orthogonal Partial Least Squares Discrimination Analysis; KEGG; Kyoto Encyclopedia of Genes and Genomes.

Ethical Statement

All experiments were performed following the Experimental Animal Ethics Committee of the Guangzhou University of Chinese Medicine (SCK(YUE) 20180085) and in accordance with the Guide for the Care and Use of Laboratory Animals of the Guangdong Provincial Government.

Author Contributions

All authors made a significant contribution to the work reported, whether that is in the conception, study design, execution, acquisition of data, analysis and interpretation, or in all these areas; took part in drafting, revising or critically reviewing the article; gave final approval of the version to be published; have agreed on the journal to which the article has been submitted; and agree to be accountable for all aspects of the work.

Funding

This research was funded by the key area special project of the "serving rural revitalization plan" of colleges and universities in Guangdong Province: construction of science and technology service system of the Southern pharmaceutical industry based on Rural Revitalization of Guangdong Province, grant number 2019KZDZX2017; Guangdong Provincial Rural Revitalization Strategy special project—Guangdong modern southern medicine industry technology system innovation team, grant number 2022KJ148; and the research project of Guangdong Provincial Bureau of Traditional Chinese Medicine—study on Rubia alcohol extract in the treatment of rheumatoid arthritis by regulating intestinal flora and restoring Treg/Th17, grant number 20221121.

Disclosure

The authors report no conflicts of interest in this work.

References

1. Bungau SG, Behl T, Singh A, et al. Targeting probiotics in rheumatoid arthritis. *Nutrients*. 2021;13(10):3376. doi:10.3390/nu13103376
2. Conforti A, Di Cola I, Pavlych V, et al. Beyond the joints, the extra-articular manifestations in rheumatoid arthritis. *Autoimmun Rev*. 2021;20(2):102735. doi:10.1016/j.autrev.2020.102735
3. Marcucci E, Bartoloni E, Alunno A, et al. Extra-articular rheumatoid arthritis. *Reumatismo*. 2018;70(4):212–224. doi:10.4081/reumatismo.2018.1106
4. Giannini D, Antonucci M, Petrelli F, Bilia S, Alunno A, Puxeddu I. One year in review 2020: pathogenesis of rheumatoid arthritis. *Clin Exp Rheumatol*. 2020;38(3):387–397.
5. van der Woude D, van der Helm-van Mil AHM. Update on the epidemiology, risk factors, and disease outcomes of rheumatoid arthritis. *Best Pract Res Clin Rheumatol*. 2018;32(2):174–187. doi:10.1016/j.berh.2018.10.005

6. Lin YJ, Anzaghe M, Schülke S. Update on the pathomechanism, diagnosis, and treatment options for rheumatoid arthritis. *Cells*. 2020;9(4). doi:10.3390/cells9040880
7. Fraenkel L, Bathon JM, England BR, et al. 2021 American college of rheumatology guideline for the treatment of rheumatoid arthritis. *Arthritis Care Res*. 2021;73(7):924–939. doi:10.1002/acr.24596
8. Bindu S, Mazumder S, Bandyopadhyay U. Non-steroidal anti-inflammatory drugs (NSAIDs) and organ damage: a current perspective. *Biochem Pharmacol*. 2020;180:114147. doi:10.1016/j.bcp.2020.114147
9. Smolen JS, Aletaha D, McInnes IB. Rheumatoid arthritis. *Lancet*. 2016;388(10055):2023–2038. doi:10.1016/S0140-6736(16)30173-8
10. Li XZ, Zhang SN. Herbal compounds for rheumatoid arthritis: literatures review and cheminformatics prediction. *Phytother Res*. 2020;34(1):51–66. doi:10.1002/ptr.6509
11. Yang P, Qian F, Zhang M, et al. Zishen tongluo formula ameliorates collagen-induced arthritis in mice by modulation of Th17/Treg balance. *J Ethnopharmacol*. 2020;250:112428. doi:10.1016/j.jep.2019.112428
12. Liu M, Liu S, Zhang Q, et al. Curculigoside attenuates oxidative stress and osteoclastogenesis via modulating Nrf2/NF-κB signaling pathway in RAW264.7 cells. *J Ethnopharmacol*. 2021;275:114129. doi:10.1016/j.jep.2021.114129
13. Wu X, Shou Q, Chen C, et al. An herbal formula attenuates collagen-induced arthritis via inhibition of JAK2-STAT3 signaling and regulation of Th17 cells in mice. *Oncotarget*. 2017;8(27):44242–44254. doi:10.18632/oncotarget.17797
14. Li HJ, Zhang CT, Du H, et al. Chemical composition of bawei Longzuan granule and its anti-arthritic activity on collagen-induced arthritis in rats by inhibiting inflammatory responses. *Chem Biodivers*. 2019;16(9):e1900294. doi:10.1002/cbdv.201900294
15. Wen M, Chen Q, Chen W, et al. A comprehensive review of Rubia cordifolia L.: traditional uses, phytochemistry, pharmacological activities, and clinical applications. *Front Pharmacol*. 2022;13:965390. doi:10.3389/fphar.2022.965390
16. Chandraker SK, Lal M, Khanam F, Dhruve P, Singh RP, Shukla R. Therapeutic potential of biogenic and optimized silver nanoparticles using Rubia cordifolia L. leaf extract. *Sci Rep*. 2022;12(1):8831. doi:10.1038/s41598-022-12878-y
17. Chandrashekar BS, Prabhakara S, Mohan T, et al. Characterization of Rubia cordifolia L. root extract and its evaluation of cardioprotective effect in Wistar rat model. *Indian J Pharmacol*. 2018;50(1):12–21. doi:10.4103/ijp.IJP_418_17
18. Shen CH, Liu CT, Song XJ, et al. Evaluation of analgesic and anti-inflammatory activities of Rubia cordifolia L. by spectrum-effect relationships. *J Chromatogr B Analyt Technol Biomed Life Sci*. 2018;1090:73–80. doi:10.1016/j.jchromb.2018.05.021
19. Zheng Z, Li S, Zhong Y, et al. UPLC-QTOF-MS identification of the chemical constituents in rat plasma and urine after oral administration of Rubia cordifolia L. extract. *Molecules*. 2017;22(8):1327. doi:10.3390/molecules22081327
20. Garcia-Carbonell R, Divakaruni AS, Lodi A, et al. Critical role of glucose metabolism in rheumatoid arthritis fibroblast-like synoviocytes. *Arthritis Rheumatol*. 2016;68(7):1614–1626. doi:10.1002/art.39608
21. Seki M, Kawai Y, Ishii C, Yamanaka T, Odawara M, Inazu M. Functional analysis of choline transporters in rheumatoid arthritis synovial fibroblasts. *Mod Rheumatol*. 2017;27(6):995–1003. doi:10.1080/14397595.2017.1280118
22. McGaha TL, Huang L, Lemos H, et al. Amino acid catabolism: a pivotal regulator of innate and adaptive immunity. *Immunol Rev*. 2012;249 (1):135–157. doi:10.1111/j.1600-065X.2012.01149.x
23. Su J, Li S, Chen J, et al. Glycerophospholipid metabolism is involved in rheumatoid arthritis pathogenesis by regulating the IL-6/JAK signaling pathway. *Biochem Biophys Res Commun*. 2022;600:130–135. doi:10.1016/j.bbrc.2022.02.003
24. Carlson AK, Rawle RA, Wallace CW, et al. Global metabolomic profiling of human synovial fluid for rheumatoid arthritis biomarkers. *Clin Exp Rheumatol*. 2019;37(3):393–399.
25. Sperling RI, Coblyn JS, Larkin JK, Benincaso AI, Austen KF, Weinblatt ME. Inhibition of leukotriene B4 synthesis in neutrophils from patients with rheumatoid arthritis by a single oral dose of methotrexate. *Arthritis Rheum*. 1990;33(8):1149–1155. doi:10.1002/art.1780330815
26. Koal T, Deigner HP. Challenges in mass spectrometry based targeted metabolomics. *Curr Mol Med*. 2010;10(2):216–226. doi:10.2174/156652410790963312
27. Zhang AH, Qiu S, Xu HY, Sun H, Wang XJ. Metabolomics in diabetes. *Clin Chim Acta*. 2014;429:106–110. doi:10.1016/j.cca.2013.11.037
28. Hicks LC, Ralphs SJ, Williams HR. Metabonomics and diagnostics. *Methods Mol Biol*. 2015;1277:233–244.
29. Kibble M, Saarinen N, Tang J, Wennerberg K, Mäkelä S, Aittokallio T. Network pharmacology applications to map the unexplored target space and therapeutic potential of natural products. *Nat Prod Rep*. 2015;32(8):1249–1266. doi:10.1039/C5NP00005J
30. Sykora T, Babal P, Mikus-Kuracinova K, et al. Hyperbilirubinemia maintained by chronic supplementation of unconjugated bilirubin improves the clinical course of experimental autoimmune arthritis. *Int J Mol Sci*. 2021;22(16):8662. doi:10.3390/ijms22168662
31. Li J, Zhong J, Huang C, Guo J, Wang B. Integration of traditional Chinese medicine and nibble debridement and dressing method reduces thrombosis and inflammatory response in the treatment of thromboangiitis obliterans. *Ann Transl Med*. 2021;9(18):1413. doi:10.21037/atm-21-3752
32. Mohamed EA, Ahmed HI, Zaky HS, Badr AM. Sesame oil mitigates memory impairment, oxidative stress, and neurodegeneration in a rat model of Alzheimer's disease. A pivotal role of NF-κB/p38MAPK/BDNF/PPAR-γ pathways. *J Ethnopharmacol*. 2021;267:113468. doi:10.1016/j.jep.2020.113468
33. Yang F, Liu M, Qin N, et al. Lipidomics coupled with pathway analysis characterizes serum metabolic changes in response to potassium oxonate induced hyperuricemic rats. *Lipids Health Dis*. 2019;18(1):112. doi:10.1186/s12944-019-1054-z
34. Liu J, Liu J, Tong X, et al. Network pharmacology prediction and molecular docking-based strategy to discover the potential pharmacological mechanism of Huai Hua San against ulcerative colitis. *Drug Des Devel Ther*. 2021;15:3255–3276. doi:10.2147/DDDT.S319786
35. Wu N, Yuan T, Yin Z, et al. Network pharmacology and molecular docking study of the Chinese Miao medicine sidaxue in the treatment of rheumatoid arthritis. *Drug Des Devel Ther*. 2022;16:435–466. doi:10.2147/DDDT.S330947
36. Pan HT, Xi ZQ, Wei XQ, Wang K. A network pharmacology approach to predict potential targets and mechanisms of "Ramulus Cinnamomi (cassiae) - Paeonia lactiflora" herb pair in the treatment of chronic pain with comorbid anxiety and depression. *Ann Med*. 2022;54(1):413–425. doi:10.1080/07853890.2022.2031268
37. Ferreira LG, Dos Santos RN, Oliva G, Andricopulo AD. Molecular docking and structure-based drug design strategies. *Molecules*. 2015;20 (7):13384–13421. doi:10.3390/molecules200713384
38. Sigsgaard I, Almdal T, Hansen BA, Vilstrup H. Dexamethasone increases the capacity of urea synthesis time dependently and reduces the body weight of rats. *Liver*. 1988;8(4):193–197. doi:10.1111/j.1600-0676.1988.tb00992.x

39. Castro-Santos P, Díaz-Peña R. Genetics of rheumatoid arthritis: a new boost is needed in Latin American populations. *Rev Bras Reumatol Engl Ed*. 2016;56(2):171–177. doi:10.1016/j.rbre.2015.10.004
40. Guo S, Zhu Q, Jiang T, et al. Genome-wide DNA methylation patterns in CD4+ T cells from Chinese Han patients with rheumatoid arthritis. *Mod Rheumatol*. 2017;27(3):441–447. doi:10.1080/14397595.2016.1218595
41. Bendele A. Animal models of rheumatoid arthritis. *J Musculoskelet Neuronal Interact*. 2001;1(4):377–385.
42. Choudhary N, Bhatt LK, Prabhavalkar KS. Experimental animal models for rheumatoid arthritis. *Immunopharmacol Immunotoxicol*. 2018;40 (3):193–200. doi:10.1080/08923973.2018.1434793
43. Brennan FM, McInnes IB. Evidence that cytokines play a role in rheumatoid arthritis. *J Clin Invest*. 2008;118(11):3537–3545. doi:10.1172/JCI36389
44. Siebert S, Tsoukas A, Robertson J, McInnes I. Cytokines as therapeutic targets in rheumatoid arthritis and other inflammatory diseases. *Pharmacol Rev*. 2015;67(2):280–309. doi:10.1124/pr.114.009639
45. McInnes IB, Schett G. Pathogenetic insights from the treatment of rheumatoid arthritis. *Lancet*. 2017;389(10086):2328–2337. doi:10.1016/S0140-6736(17)31472-1
46. Maini RN, Breedveld FC, Kalden JR, et al. Sustained improvement over two years in physical function, structural damage, and signs and symptoms among patients with rheumatoid arthritis treated with infliximab and methotrexate. *Arthritis Rheum*. 2004;50(4):1051–1065. doi:10.1002/art.20159
47. Keystone EC, Kavanaugh AF, Sharp JT, et al. Radiographic, clinical, and functional outcomes of treatment with Adalimumab (a human anti-tumor necrosis factor monoclonal antibody) in patients with active rheumatoid arthritis receiving concomitant methotrexate therapy: a randomized, placebo-controlled, 52-week trial. *Arthritis Rheum*. 2004;50(5):1400–1411. doi:10.1002/art.20217
48. Emery P, Fleischmann RM, Moreland LW, et al. Golimumab, a human anti-tumor necrosis factor alpha monoclonal antibody, injected subcutaneously every four weeks in methotrexate-naive patients with active rheumatoid arthritis: twenty-four-week results of a Phase III, multicenter, randomized, double-blind, placebo-controlled study of golimumab before methotrexate as first-line therapy for early-onset rheumatoid arthritis. *Arthritis Rheum*. 2009;60(8):2272–2283. doi:10.1002/art.24638
49. Rubbert-Roth A, Atzeni F, Masala IF, Caporali R, Montecucco C, Sarzi-Puttini P. TNF inhibitors in rheumatoid arthritis and spondyloarthritis: are they the same? *Autoimmun Rev*. 2018;17(1):24–28. doi:10.1016/j.autrev.2017.11.005
50. Lopez-Castejon G, Brough D. Understanding the mechanism of IL-1β secretion. *Cytokine Growth Factor Rev*. 2011;22(4):189–195. doi:10.1016/j.cytogfr.2011.10.001
51. Ling Y, Yang J, Hua D, et al. ZhiJingSan inhibits osteoclastogenesis via regulating RANKL/NF-κB signaling pathway and ameliorates bone erosion in collagen-induced mouse arthritis. *Front Pharmacol*. 2021;12:693777. doi:10.3389/fphar.2021.693777
52. Saccani S, Marazzi I, Beg AA, Natoli G. Degradation of promoter-bound p65/RelA is essential for the prompt termination of the nuclear factor kappaB response. *J Exp Med*. 2004;200(1):107–113. doi:10.1084/jem.20040196
53. Rahman MM, McFadden G. Modulation of NF-κB signalling by microbial pathogens. *Nat Rev Microbiol*. 2011;9(4):291–306. doi:10.1038/nrmicro2539
54. Gomez PF, Pillinger MH, Attur M, et al. Resolution of inflammation: prostaglandin E2 dissociates nuclear trafficking of individual NF-kappaB subunits (p65, p50) in stimulated rheumatoid synovial fibroblasts. *J Immunol*. 2005;175(10):6924–6930. doi:10.4049/jimmunol.175.10.6924
55. McMurray HF, Parthasarathy S, Steinberg D. Oxidatively modified low density lipoprotein is a chemoattractant for human T lymphocytes. *J Clin Invest*. 1993;92(2):1004–1008. doi:10.1172/JCI116605
56. Liu P, Zhu W, Chen C, et al. The mechanisms of lysophosphatidylcholine in the development of diseases. *Life Sci*. 2020;247:117443. doi:10.1016/j.lfs.2020.117443
57. Hegen M, Sun L, Uozumi N, et al. Cytosolic phospholipase A2alpha-deficient mice are resistant to collagen-induced arthritis. *J Exp Med*. 2003;197 (10):1297–1302. doi:10.1084/jem.20030016
58. Ding X, Hu J, Li J, et al. Metabolomics analysis of collagen-induced arthritis in rats and interventional effects of oral tolerance. *Anal Biochem*. 2014;458:49–57. doi:10.1016/j.ab.2014.04.035
59. Liu NJ, Chapman R, Lin Y, et al. Point of care testing of phospholipase A2 group IIA for serological diagnosis of rheumatoid arthritis. *Nanoscale*. 2016;8(8):4482–4485. doi:10.1039/C5NR08423G
60. Margarucci L, Monti MC, Chini MG, et al. The inactivation mechanism of human group IIA phospholipase A(2) by Scalaradial. *Chembiochem*. 2012;13(15):2259–2264. doi:10.1002/cbic.201200453
61. Qian Q, Gao Y, Xun G, et al. Synchronous investigation of the mechanism and substance basis of tripterygium glycosides tablets on anti-rheumatoid arthritis and hepatotoxicity. *Appl Biochem Biotechnol*. 2022;194(11):5333–5352. doi:10.1007/s12010-022-04011-6
62. Ackerman SJ, Liu L, Kwatia MA, et al. Charcot-Leyden crystal protein (galectin-10) is not a dual function galectin with lysophospholipase activity but binds a lysophospholipase inhibitor in a novel structural fashion. *J Biol Chem*. 2002;277(17):14859–14868. doi:10.1074/jbc.M200221200
63. Rodríguez-Alcázar JF, Ataide MA, Engels G, et al. Charcot-leyden crystals activate the NLRP3 inflammasome and cause IL-1β inflammation in human macrophages. *J Immunol*. 2019;202(2):550–558. doi:10.4049/jimmunol.1800107
64. Kargili A, Bavbek N, Kaya A, Koşar A, Karaaslan Y. Eosinophilia in rheumatologic diseases: a prospective study of 1000 cases. *Rheumatol Int*. 2004;24(6):321–324. doi:10.1007/s00296-004-0469-6
65. Emmanuel D, Parija SC, Jain A, Misra DP, Kar R, Negi VS. Persistent eosinophilia in rheumatoid arthritis: a prospective observational study. *Rheumatol Int*. 2019;39(2):245–253. doi:10.1007/s00296-018-4191-1
66. Peres RS, Santos GB, Cecilio NT, et al. Lapachol, a compound targeting pyrimidine metabolism, ameliorates experimental autoimmune arthritis. *Arthritis Res Ther*. 2017;19(1):47. doi:10.1186/s13075-017-1236-x
67. Yu S, Li X, Guo X, Zhang H, Qin R, Wang M. UCK2 upregulation might serve as an indicator of unfavorable prognosis of hepatocellular carcinoma. *IUBMB Life*. 2019;71(1):105–112. doi:10.1002/iub.1941
68. Malami I, Abdul AB, Abdullah R, et al. Crude extracts, flavokawain B and alpinetin compounds from the rhizome of alpinia mutica induce cell death via UCK2 enzyme inhibition and in turn reduce 18S rRNA biosynthesis in HT-29 cells. *PLoS One*. 2017;12(1):e0170233. doi:10.1371/journal.pone.0170233
69. Stancíková M, Rovenský J. Effect of cyclosporin on the activity of cytidine deaminase and adenosine deaminase in the serum and polymorphonuclear leukocytes of patients with rheumatoid arthritis. *Int J Tissue React*. 1993;15(4):169–174.

70. Rampazzo C, Kost-Alimova M, Ruzzenente B, Dumanski JP, Bianchi V. Mouse cytosolic and mitochondrial deoxyribonucleotidases: cDNA cloning of the mitochondrial enzyme, gene structures, chromosomal mapping and comparison with the human orthologs. *Gene*. 2002;294(1–2):109–117. doi:10.1016/S0378-1119(02)00651-0
71. Biswas N, Rodriguez-Garcia M, Crist SG, et al. Effect of tenofovir on nucleotidases and cytokines in HIV-1 target cells. *PLoS One*. 2013;8(10):e78814. doi:10.1371/journal.pone.0078814
72. Fosso MY, Chan KY, Gregory R, Chang CW. Library synthesis and antibacterial investigation of cationic anthraquinone analogs. *ACS Comb Sci*. 2012;14(3):231–235. doi:10.1021/co2002075
73. Davis RH, Agnew PS, Shapiro E. Antiarthritic activity of anthraquinones found in aloe for podiatric medicine. *J Am Podiatr Med Assoc*. 1986;76(2):61–66.
74. Müller-Lissner SA. Adverse effects of laxatives: fact and fiction. *Pharmacology*. 1993;47(Suppl 1):138–145. doi:10.1159/000139853
75. Haoudar A, Chekhlabi N, El Kettani C, Dini N. Acute hepatitis and pancytopenia in a child with chronic abuse of senna. *Cureus*. 2021;13(1):e12436. doi:10.7759/cureus.12436
76. Seybold U, Landauer N, Hillebrand S, Goebel FD. Senna-induced hepatitis in a poor metabolizer. *Ann Intern Med*. 2004;141(8):650–651. doi:10.7326/0003-4819-141-8-200410190-00024